ADVANCED FUNCTIONAL MATERIALS
www.afm-journal.de

Ultrastretchable Fibers with Metallic Conductivity Using a Liquid Metal Alloy Core

*Shu Zhu, Ju-Hee So, Robin Mays, Sharvil Desai, William R. Barnes, Behnam Pourdeyhimi, and Michael D. Dickey**

The fabrication and characterization of fibers that are ultrastretchable and have metallic electrical conductivity are described. The fibers consist of a liquid metal alloy, eutectic gallium indium (EGaIn), injected into the core of stretchable hollow fibers composed of a triblock copolymer, poly[styrene-*b*-(ethylene-*co*-butylene)-*b*-styrene] (SEBS) resin. The hollow fibers are easy to mass-produce with controlled size using commercially available melt processing methods. The fibers are similar to conventional metallic wires, but can be stretched orders of magnitude further while retaining electrical conductivity. Mechanical measurements with and without the liquid metal inside the fibers show the liquid core has a negligible impact on the mechanical properties of the fibers, which is in contrast to most conductive composite fibers. The fibers also maintain the same tactile properties with and without the metal. Electrical measurements show that the fibers increase resistance as the fiber elongates and the cross sectional area narrows. Fibers with larger diameters change from a triangular to a more circular cross-section during stretching, which has the appeal of lowering the resistance below that predicted by theory. To demonstrate their utility, the ultrastretchable fibers are used as stretchable wires for earphones and for a battery charger and perform as well as their conventional parts.

1. Introduction

This paper describes the fabrication and characterization of ultra-stretchable fibers with metallic conductivity formed by injecting a moldable liquid metal into hollow elastomeric fibers. We fabricated the hollow fibers by melt processing commercial a thermoplastic elastomer (Kraton G1643). Injecting a liquid metal alloy, eutectic gallium indium (EGaIn, 75% Ga, 25% In by weight, melting point 15.7 °C[1,2]), into these fibers produces conductive wires encased in an insulating polymer shell. Because the metal is a liquid at room temperature, it flows and maintains metallic conductivity while stretching the fibers significantly (up to ≈700% strain). Stretchable and flexible conductive fibers may be useful for incorporating electronic function into non-rigid substrates (e.g., textiles, filters, clothing, paper, and sensors).[3–5]

A number of flexible electronic devices, including flexible circuits, waveguides, and epidermal electronics have been fabricated from rigid materials that are rendered flexible by using a thin form factor.[6–8] Coercing these thin films into wavy shapes on elastomeric substrates offers a route to make them stretchable and thus, more durable in mechanically demanding applications. An alternative approach for stretchable electronics is to use intrinsically stretchable conductors such as conductive pastes (e.g., pastes of carbon nanotubes or metal particles), composites, or liquids.[9–11] These stretchable conductors are useful for wires, interconnects, metamaterials, and antennas.

Conductive fibers are an attractive platform for flexible and stretchable electronics because fibers are inexpensive, inherently flexible, can be formed into 2D and 3D fabrics, and can be mass produced via melt processing with very high speeds (>1000 m/min). The most common methods to impart conductivity into melt processed fibers include coating the fibers with conductive films (e.g., metals or carbon)[12–14] or creating conductive composites by introducing electrically conductive additives (e.g., graphite or carbon,[15–18] metal nanoparticles,[19] conductive polymers[17,20–23] such as polyaniline and poly-3-hexylthiophene). To ensure conductivity through the fiber, a composite fiber requires the addition of a sufficient amount of an additive to reach percolation. Thus, the mechanical properties (modulus, toughness, tactility, yield point) of the fiber may change in unintended ways; coating methods have similar effects. Moreover, the composite fibers rarely result in metallic conductivity and conductive polymers tend to degrade due to oxidation.[12,24] Also, in some applications (e.g., commercial wires), it may be undesirable to have the current carrying components exposed to the exterior of the fiber. Commercial wires (e.g., copper wire insulated with polymer) are flexible due to

S. Zhu, J.-H. So, R. L. Mays, Dr. S. Desai, Prof. M. D. Dickey
Department of Chemical and Biomolecular Engineering
North Carolina State University
911 Partners Way, Raleigh, NC 27695, USA
E-mail: michael_dickey@ncsu.edu
W. R. Barnes, Prof. B. Pourdeyhimi,
The Nonwovens Institute,
North Carolina State University,
1000 Main Campus Dr., Raleigh, NC 27606, USA

DOI: 10.1002/adfm.201202405

their thin cross-section, but are not stretchable.[25,26] We sought to demonstrate a new approach to create conductive fibers that would be simple, highly conductive, and stretchable without modifying the mechanical or tactile properties of the fiber. The present work is distinguished by 1) the ability of the fibers to maintain metallic conductivity with ultralarge strains; 2) the geometry of the fiber (a conductive core surrounded by an insulating shell, which is similar to conventional wires); and 3) the mechanical and tactile properties of the fiber, which are altered minimally since the fiber shell is unadulterated polymer.

We fabricated the fibers by injecting a moldable liquid metal into hollow fibers. The metal, EGaIn, is liquid at room temperature with a low viscosity and a high conductivity ($\sigma = 3.4 \times 10^4$ S/cm[27]). The liquid metal forms spontaneously a thin oxide skin at room temperature that reforms rapidly when ruptured. The metal can be injected into capillaries, microchannels, and hollow fibers by exceeding the pressure required to rupture the skin.[2] Once it is in the capillary, a new skin forms rapidly and holds it into place. This ability to mold the metal into non-spherical shapes has been utilized to fabricate microelectrodes,[28] stretchable antennas,[11,29,30] stretchable interconnects and conductors,[31,32] soft diodes,[33] and flexible solar cells.[34] Here, we harness this property to demonstrate ultrastretchable, conductive wires inside hollow elastomeric fibers.

Poly[styrene-*b*-(ethylene-*co*-butylene)-*b*-styrene] (SEBS) resin is a thermoplastic elastomer with low modulus, high tensile strength (stress at break ≈10 MPa), high stretchability, and good resistance to most chemicals.[35] SEBS resins are used widely in the production of handles and grips, medical equipment, roofing and many other applications due to their rubber-like properties. We chose a particular type of SEBS resin, Kraton G1643 because it is commercially available, highly stretchable (strain at break >900%) and easy to melt process. This particular resin consists of 20% styrene endblocks and 80% ethylene-butylene midblock[35] and gel permeation chromatography shows it to have a number average molecular weight (M_n) of 116 000 and a weight average molecular weight (M_w) of 139 000 with a polydispersity index (PDI) of 1.19. Here, we describe the fabrication and characterization of stretchable conductive fibers and demonstrate their function as a stretchable charger and as a stretchable cable for earphones.

2. Results

We produced hollow fibers by melt extruding SEBS through a die consisting of a circular slit divided into three equal segments. As the polymer exits the slits and as it is drawn, it flows and forms a hollow fiber. The fibers exited the extruder in a downward motion (i.e., in the direction of gravity) and a collection roller dictated the speed with which the fibers were drawn through a water bath at room temperature. To control the dimensions of the hollow fibers, we varied the spinning rate of the collection roller. **Figure 1** shows the cross sectional dimensions of the fibers for spinning rates ranging from 25 to 1000 m/min (dimensions for free-fall fibers appear in Figure 1b at 0 m/min). In all cases, the fibers have a triangular cross section, which is most likely due to the geometry of the die. The inner diameter of the fabricated fiber varied from 360 to

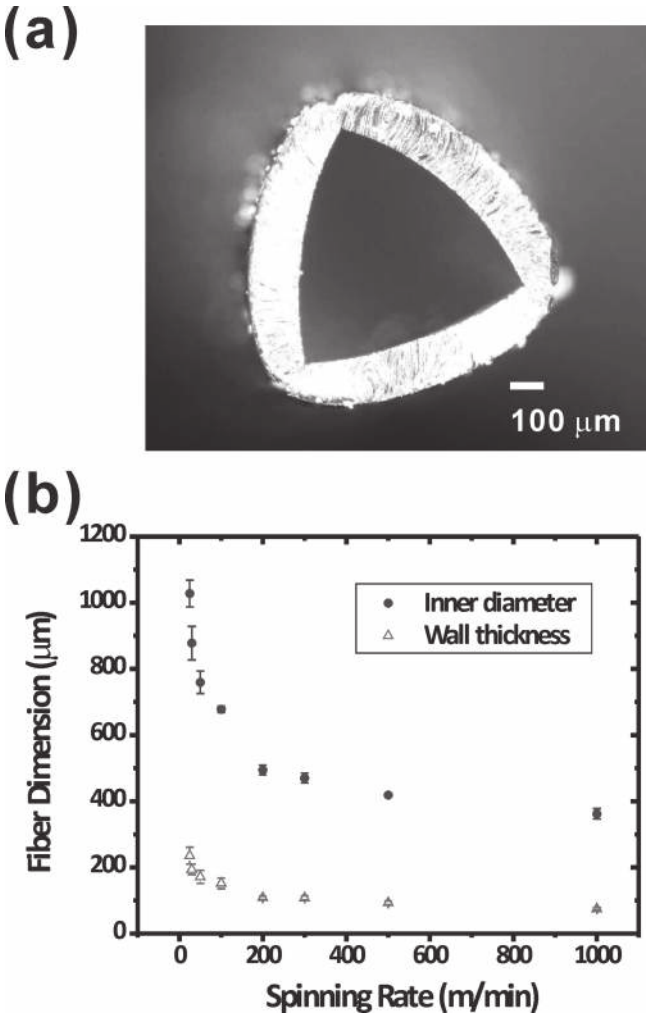

Figure 1. a) Optical image of the cross-section of a hollow fiber formed at 100 m/min. b) The inner diameter (ID) and wall thickness (WT) of the fibers decreased with increased spinning rate.

1030 μm (we define the inner diameter as the average of the lengths of the three lines that originate from the vertexes and bisect the triangular cross-section of the core of the fiber) and the thickness of the walls of the fiber ranges from 75 to 240 μm. As expected, faster spinning rates produced smaller fibers since the extruder kept the mass flow rate constant. The outer diameter of the fibers appears to level out at higher spinning rates. We varied the quench distance (i.e., the distance between the die and the water bath), but did not observe significant changes in fiber geometry (±25 μm over all distances allowed by the experimental setup).

It is straightforward to inject the metal into the hollow fibers. A long segment of hollow fiber can be filled with liquid metal using a syringe and then cut into several pieces with desired lengths. The longest segment we attempted to fill was ≈1 m long and it filled easily. Injecting the metal requires overcoming the interfacial forces, which scale inversely with the diameter of the fibers.[2] Pressures of ≈0.1 atm are sufficient to overcome these forces for the dimensions of fibers used in this study. The pressure required to overcome viscous drag is only

Adv. Funct. Mater. 2013,
DOI: 10.1002/adfm.201202405

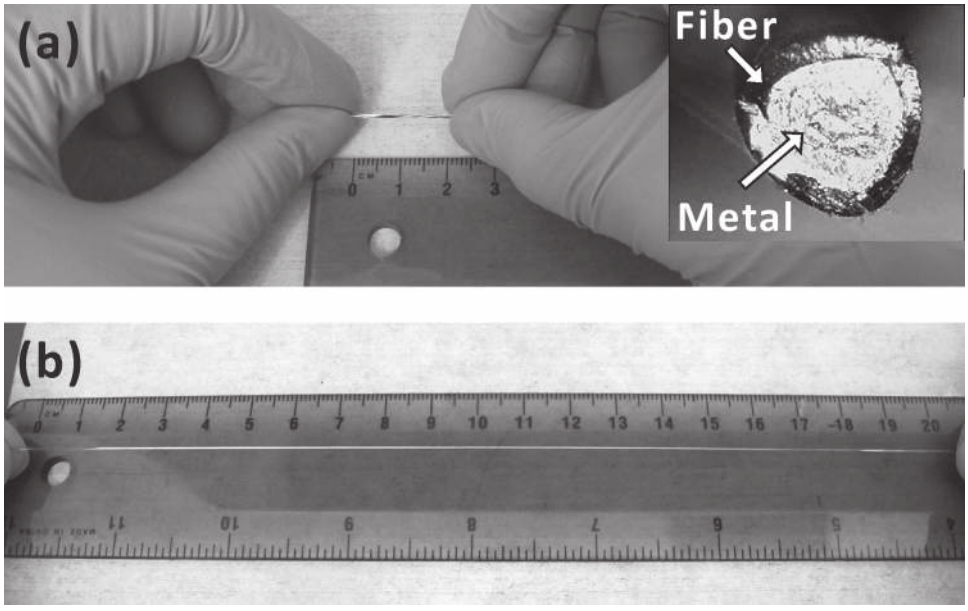

Figure 2. a) A relaxed, 2 cm section of an ultrastretchable conductive fiber. The shiny core of its cross-section (inset) is the liquid metal. b) The fiber is stretched to 20 cm and the metal appears to uniformly fill the stretched fiber.

significant at large injection velocities or long lengths of fiber due to the low viscosity of the metal. The oxidized skin of the metal prevents the metal from flowing out of the fiber when the fiber is not disturbed (e.g., squeezed significantly). The inset in **Figure 2**a shows that the metal remains flush with the cut end of the fiber.

We hypothesized that the incorporation of the metal impacts minimally the mechanical properties of the fibers since the metal is a low viscosity liquid and flows readily in response to applied strain. An extensometer measured the mechanical properties of both the hollow and filled fibers. **Figure 3** shows the stress–strain profiles of the fibers for two spinning rates

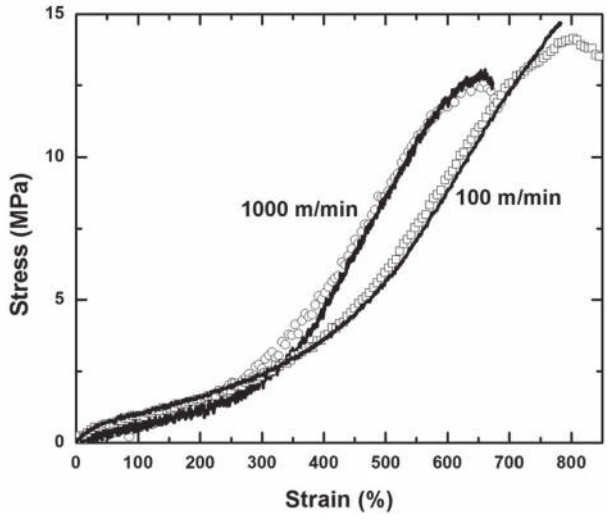

Figure 3. The stress–strain plots of elastomeric hollow (hollow symbols) and filled (solid lines) fibers with two different spinning rates. The fibers have the same mechanical properties with and without the metal.

spanning an order of magnitude in spin speed (100 m/min and 1000 m/min). The plots show the typical properties of thermoplastic elastomers: low modulus and high tensile strength. Although the fibers have very similar mechanical properties, as expected, fibers made with the lowest spinning rate can be strained the furthest before the point of failure. At the lowest spinning rate (100 m/min), we found that the fibers could be stretched to 800–1000% strain before reaching the point of failure. Figure 3 shows that the fibers with and without the metal have nearly identical mechanical properties, which illustrates the negligible effects of the liquid metal on the mechanical properties of the fibers.

For many applications, a practical consideration is the effect of multiple strain cycles on the performance of the fiber. We performed cyclic testing on the fibers produced at 1000 m/min to quantify the effects of repeated strain on the mechanical properties. **Figure 4**a shows that after the first cycle (0 to 800 to 0% strain), subsequent strain cycles overlap nearly perfectly with minimal signs of hysteresis. After the first cycle, there is ≈50% unrecoverable strain (i.e., the "set"), which does not change with subsequent cycles. This result suggests there is some plastic deformation during the first strain cycle, but negligible plastic deformation during subsequent cycles. Fibers fabricated with other spinning rates showed similar behavior. We also performed cyclic testing on the fibers at lower amounts of strain (0 to 50 to 0% strain), which may be more representative of strains encountered in actual applications (e.g., textiles). At these strain cycles, there is only ≈5% unrecoverable strain (Figure 4b). At extreme levels of strain (i.e., 800%), the fibers produced at 1000 m/min broke after 20–40 cycles. The durability improved for fibers produced at 100 m/min, which broke typically after 80–100 cycles at 800% strain. At intermediate strains (i.e., 50% and 400% strain), the fibers did not break after hundreds of cycles.

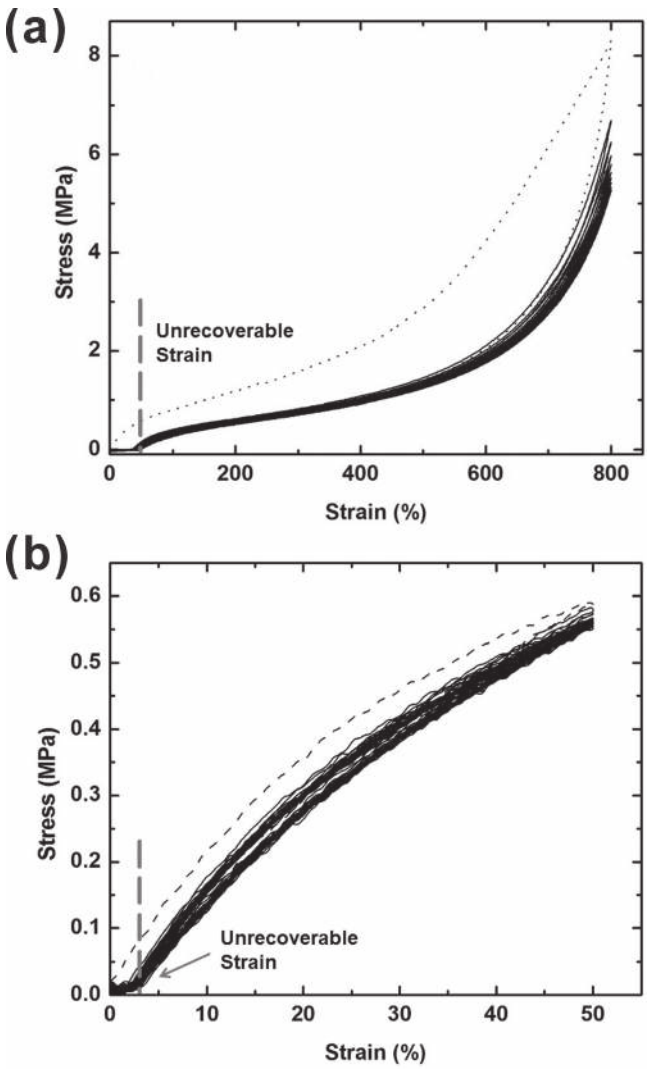

Figure 4. Cyclic tests of the mechanical properties of the hollow fibers fabricated with a spinning rate of 1000 m/min at a) 800% and b) 50% strain. The first cycle is indicated with a dashed line and subsequent cycles are solid lines. A vertical line marks the amount of unrecoverable strain resulting from plastic deformation.

The electrical resistance of the fiber should increase as a function of applied strain since the length of the fiber increases while the cross-sectional area decreases. We measured the resistance as a function of strain and normalized all measurements by the resistance at zero strain such that the initial normalized resistance is 1. The resistance R of a wire depends on its resistivity ρ, length L, and cross-sectional area A, as described in Pouillet's law. Assuming that the polymer sheath has a Poisson's ratio of 0.5 and the metal is incompressible, then the resistance of the fiber should be proportional to the change in the square of the length based solely on geometry. We developed two sets of theoretical resistance values: one is based on the assumption that the cross-sectional area remains triangular while stretching and the other one assumes it becomes circular (i.e., for a given circumference, the cross-sectional area for a circle is 65% larger than an equilateral triangle and thus, the resistance through a circular cross section should be lower). The experimental data, in principle, should be within these bounds for the given assumptions.

Figure 5 shows that the resistance increases as a function of strain. The fibers with a smaller cross sectional area (1000 m/min) have an electrical resistance that agrees nearly perfectly with that predicted by the model for a triangular cross-sectional area. The resistance of these fibers increases dramatically beyond the last plotted point (≈600% strain). The fibers with a larger cross sectional area (100 m/min) initially have an electrical resistance similar to the theoretical resistance for a triangular cross section but then deviate gradually to lower values and follow the resistance prediction for a circular cross-section until 700–800% strain, at which point the resistance rises rapidly. The fibers maintained electrical continuity to ≈1000% strain, albeit at significantly higher resistances. Figure 5a represents the best case

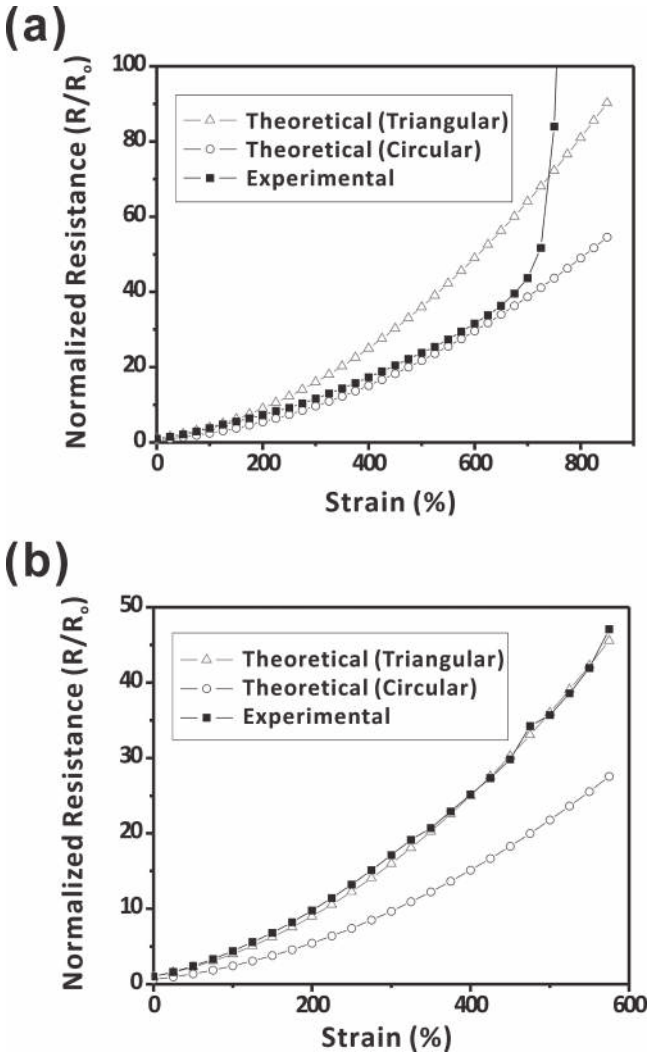

Figure 5. The experimental (filled squares) and theoretical resistance (empty triangles and circles) of conductive fibers with two different spinning rates of a) 100 and b) 1000 m/min. The triangles indicate the geometrical effects of elongation and the circles represent the effect of changes in cross-sectional geometry during elongation.

Adv. Funct. Mater. **2013**,
DOI: 10.1002/adfm.201202405

scenario; in some samples (100 m/min), the resistance would increase rapidly as low as 400% strain. The loss of conductivity coincides with the physical collapse of the fibers. The metallic conductivity recovers upon returning the fibers back to a non-stressed state (in some cases, massaging the fibers is required to regain continuity).

The geometric model captures the general trends in Figure 5 and suggests that the resistance is less than or equal to that expected from a triangular shaped fiber. We compared the cross-sectional geometry of the 100 and 1000 m/min fibers during elongation. The cross-section of the fiber with 100 m/min spinning rate appears to become circular while the fibers with 1000 m/min spinning rate maintain their triangular cross section (see Figure S1,S2 in the Supporting Information), which is consistent with the results of Figure 5. The ability of the fibers produced at 1000 m/min to maintain a triangular profile during elongation could be a result of the smaller size (i.e., increasing the circumference of the fiber should make the side walls easier to deform). Regardless of these subtle effects, the key advance of this work is the remarkable conductivity at large strains.

The fibers have a resistivity of $\approx 3 \times 10^{-5}$ Ω cm until the strain at which the resistance increases rapidly. This value is expected based on the conductivity of the metal (some papers in the literature utilize units of resistance normalized by the length of the fiber, in which case the 100 m/min and 1000 m/min fibers at 500% strain have values of 0.08 and 0.24 Ω/cm). This metallic conductivity exceeds the most conductive composite fibers in the literature (by approximately a factor of 30)[36] and the resistivity is within an order of magnitude of conventional rigid copper wires. The elongation also nearly matches some of the most stretchable conductive fibers in the literature while exceeding the conductivity by four orders of magnitude.[22]

A potential drawback of a liquid core encased in an elastomeric shell is that the metal can flow and increase its resistance when pinched. We performed some qualitative experiments to emulate conditions the fiber may encounter during handling. We intentionally pinched the 100 m/min fiber using pressure from our fingers and found the resistance to increase by an order of magnitude, but not lose electrical continuity. The resistance returned to its initial value when we stopped pinching the fiber. The resistance increased two orders of magnitude, but did not lose its electrical continuity when we concentrated the pressure using our finger nails. The resistance recovered to its pre-pinched value after releasing the force and massaging the fiber. These qualitative experiments underscore a limitation of using soft materials, yet suggest that it is challenging to completely eliminate electrical continuity by hand.

To demonstrate the utility of stretchable fibers in electronic applications, we utilized the fibers as wires of a charger and earphones for a portable music player (iPod). We cut a portion of an iPod charger line and inserted four stretchable fibers (two power wires and two data transmission wires) as shown in **Figure 6**a. We used adhesive to bond the stretchable fibers to the rigid wires of the iPod. The iPod began charging when connected to a computer through the stretchable charger, and continued charging while we repeatedly stretched and relaxed the fibers (see Video S1 in the Supporting information). We found that the stretchable charger replenished the battery at approximately the same rate as the commercial charger (see Supporting Information). We also inserted the fibers to replace a portion of the wires for earphones (Figure 6b) and the earphones continued to play music without noticeable degredation to volume or sound quality when elongated (see Video S2 in the Supporting information). We repeated several tens of cycles of stretching (≈300% strain) and relaxing the wires of the iPod charger and the earphones and their performance did not change in any apparent way. In both examples, the stretchable fibers have a lower resistance per unit length than the commercial wires and thus it is expected that there should be no degradation in performance.

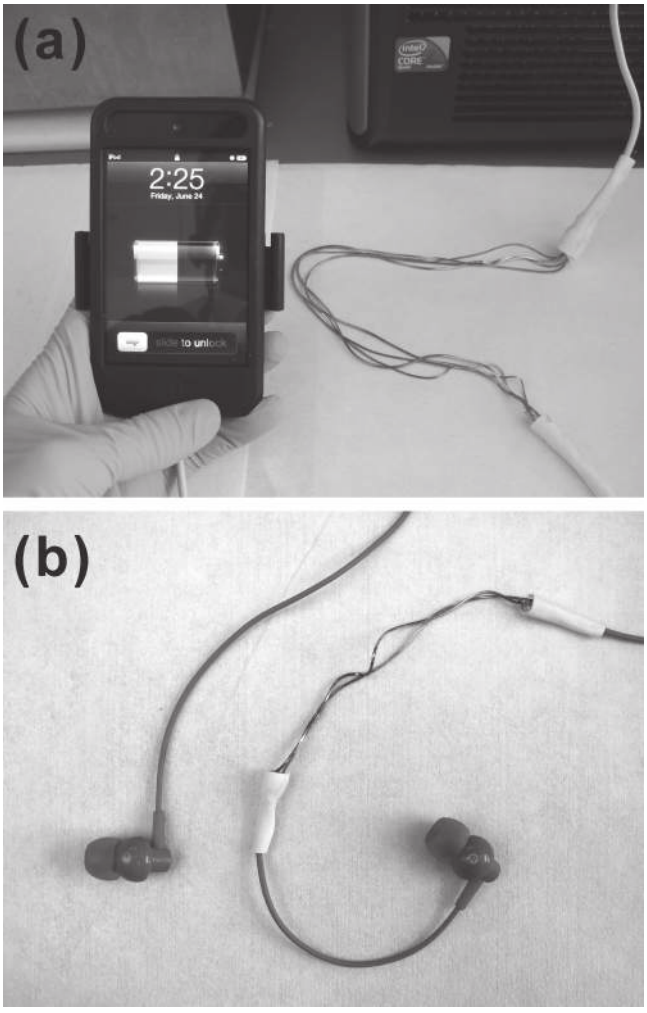

Figure 6. a) Stretchable charger for an iPod and b) stretchable cable for earphones.

3. Conclusion

This study provides an alternative approach to generate ultra-stretchable conductive fibers by simply injecting liquid alloy (EGaIn) into hollow polymeric (Kraton SEBS) fibers. The dimensions of the conductive fibers can be manipulated by varying the spinning rate of collecting rollers during the melt spinning process. The fibers have the same mechanical and tactile

properties with and without the metal. Metallic electrical continuity can be maintained to greater than 700% strain depending on the dimensions of the fiber, which we believe represents one of the best combinations of conductivity and stretchability for conductive fibers reported to date. The conductive fibers can be incorporated into numerous applications including flexible electronics, smart garments, stretchable wires, inductors, interconnects, and antennas. A limitation of this approach is the liquid core of the fibers can collapse under concentrated pressure or at large strains, although conductivity can be restored. For applications that do not require ultra-stretchability, other polymers may be more appropriate for achieving the desired mechanical stability while retaining metallic conductivity. Likewise, the mechanical properties of the fibers here are limited only by the properties of the polymer, which in principle could be rendered even more stretchable (with less hysteresis and improved durability) by the incorporation of block-selective oils.[37]

4. Experimental Section

Fabrication of Hollow Fibers: Hollow fibers were fabricated using a melt drawing process used widely in the non-wovens industry. A pilot scale Fuji Filter Melt Spinning Tester (MST-CII Special Type) was used. The instrument melt extruded the polymer resin at 230 °C and 400 psi through a hollow configured die. It was customary to use three or four slits to form hollow fibers. The die consisted of a circular slit divided into three equal sections. The circle had an outer diameter of 2 mm and inner diameter of 1.5 mm. The slits were 3 mm deep and the sections were separated by 0.2 mm. A series of rollers mechanically drew the extruded hollow fibers through a water bath at room temperature to cool the fibers and the final roller collected them and dictated the "spinning rate". The quench distance (i.e., the distance from the die to the water bath) was varied between 51 and 97 cm, and the speed of the gear pump that meters the polymer (between 20 and 47 rpm) was also varied. These changes had minimal effects on the fiber dimensions (e.g., for a draw rate of 1000 m/min, a range of diameters from 320 µm to 350 µm was observed, depending on the conditions). Taken in sum, these results suggest that other methods may be necessary to make even smaller fibers (e.g., different die dimensions).

Injection of Liquid Metal: The liquid metal was injected into the hollow fibers to fabricate stretchable conductive fibers. A needle on a syringe filled with the liquid metal and threaded into the fiber provided the source of the conductive core of conductive fibers. For cases in which the inner diameter of the needle was larger than the diameter of the fiber, the fiber was inserted into the needle and sealed with glue so that the syringe would force the metal into the fiber.

Mechanical Characterization: The mechanical properties of both hollow and filled fibers with different dimensions were measured using an Instron 5943 with a 1kN load cell. Two hydraulic grips held 1 inch sections of fiber and stretched it at a constant rate of 10 cm/min. During elongation, a computer recorded the gauge length between the two grips and converted the measured force into pressure based on the cross-sectional area of the fiber. For the cyclic testing a 10 N load cell was used, and linear velocities of 10 cm/min for the fibers drawn at 100 m/min and 3 cm/min for the fibers drawn at 1000 m/min were used to decrease the experimental noise.

Electrical Characterization: A customized digitally controlled stretcher extended the conductive fibers at 1 mm/s while measuring the resistance using a four point probe measurement. Copper wire inserted into both open ends of the fibers provided electrical connections between the liquid metal and the probe clamps from the source meter. The resistance of these wires was measured to be 13.4 mΩ, which agreed with the theoretical value based on the resistivity of copper and the physical dimensions of the wires. To prevent any slippage that might occur during fiber stretching, loose loops of the fiber were assembled at each end of the conductive fibers. The loops had a diameter of about 0.25 inch while leaving a 1 inch straight section in between the loops as the effective original sample length. A drop of glue encased the loops and the copper wire connections, and their resistance was subtracted from the overall resistance measurement to isolate the contributions from the stretchable portion of the fiber. A four point probe technique using a Keithley 2400 measured the overall resistance (through the copper wires, loops, and stretchable portion of the fiber).

Supporting Information

Supporting Information is available from the Wiley Online Library or from the author.

Acknowledgements

This work was supported by the National Science Foundation (CAREER Award CMMI-0954321) and the NSF's Research Triangle MRSEC (DMR-1121107). The authors thank Dr. Steve Smith and Prof. Rich Spontak for the GPC measurements and helpful discussions.

Received: August 22, 2012
Revised: October 29, 2012

[1] S. J. French, D. J. Saunders, G. W. Ingle, *J. Phys. Chem.* **1938**, *42*, 265.
[2] M. D. Dickey, R. C. Chiechi, R. J. Larsen, E. A. Weiss, D. A. Weitz, G. M. Whitesides, *Adv. Funct. Mater.* **2008**, *18*, 1097.
[3] R. F. Service, *Science* **2003**, *301*, 909.
[4] P. Gibbs, H. H. Asada, *J. Neuroeng. Rehabil.* **2005**, *2*, 7.
[5] D.-H. Kim, J. A. Rogers, *Adv. Mater.* **2008**, *20*, 4887.
[6] J. A. Rogers, T. Someya, Y. Huang, *Science* **2010**, *327*, 1603.
[7] D.-H. Kim, J. Xiao, J. Song, Y. Huang, J. A. Rogers, *Adv. Mater.* **2010**, *22*, 2108.
[8] R.-H. Kim, D.-H. Kim, J. Xiao, B. H. Kim, S.-I. Park, B. Panilaitis, R. Ghaffari, J. Yao, Li Ming, Z. Liu, V. Malyarchuk, D. G. Kim, A.-P. Le, R. G. Nuzzo, D. L. Kaplan, F. G. Omenetto, Y. Huang, Z. Kang, J. A. Rogers, *Nat. Mater.* **2010**, *9*, 929.
[9] K.-Y. Chun, Y. Oh, J. Rho, J.-H. Ahn, Y.-J. Kim, H. R. Choi, S. Baik, *Nat. Nanotechnol.* **2010**, *5*, 853.
[10] T. Sekitani, Y. Noguchi, K. Hata, T. Fukushima, T. Aida, T. Someya, *Science* **2008**, *321*, 1468
[11] J.-H. So, J. Thelen, A. Qusba, G. J. Hayes, G. Lazzi, M. D. Dickey, *Adv. Funct. Mater.* **2009**, *19*, 3632.
[12] X. Jin, C. Xiao, S. An, G. Jia, *J. Mater. Sci.* **2007**, *42*, 4384.
[13] N. J. Pinto, P. Carrion, J. X. Quinones, *Mater. Sci. Eng., A* **2004**, *366*, 1.
[14] D. Zabetakis, M. Dinderman, P. Schoen, *Adv. Mater.* **2005**, *17*, 734.
[15] G. Che, B. B. Lakshmi, C. R. Martin, E. R. Fisher, R. S. Ruoff, *Chem. Mater.* **1998**, *10*, 260.
[16] Z. Li, G. Luo, F. Wei, Y. Huang, *Compos. Sci. Technol.* **2006**, *66*, 1022.
[17] A. Soroudi, M. Skrifvars, *Synth. Met.* **2010**, *160*, 1143.
[18] W. Thongruang, R. J. Spontak, C. M. Balik, *Polymer* **2002**, *43*, 3717.
[19] G. Mattana, P. Cosseddu, B. Fraboni, G. G. Malliaras, J. P. Hinestroza, A. Bonfiglio, *Org. Electron.* **2011**, *12*, 2033.
[20] B. Kim, V. Koncar, E. Devaux, C. Dufour, P. Viallier, *Synth. Met.* **2004**, *146*, 167.

[21] C. R. Ríos-Soberanis, R. A. Ley-Bonilla, R. H. Cruz-Estrada, C. V. Cupul-Manzano, L. M. Rangel-Rodríguez, A. Caballero-Can, *Polym. Int.* **2009**, *58*, 817.
[22] A. J. Granero, P. Wagner, K. Wagner, J. M. Razal, G. G. Wallace, M. in het Panhuis, *Adv. Funct. Mater.* **2011**, *21*, 955.
[23] P. Sukitpaneenit, T. Thanpitcha, A. Sirivat, C. Weder, R. Rujiravanit, *J. Appl. Polym. Sci.* **2007**, *106*, 4038.
[24] J. Stejskal, I. Sapurina, J. Proke, J. Zemek, *Synth. Met.* **1999**, *105*, 195.
[25] S. P. Lacour, D. Chan, S. Wagner, T. Li, Z. Suo, *Appl. Phys. Lett.* **2006**, *88*, 204103.
[26] T. Li, Z. Huang, Z. Suo, S. P. Lacour, S. Wagner, *Appl. Phys. Lett.* **2004**, *85*, 3435.
[27] D. Zrnic, D. S. Swatik, *J. Less-Common Met.* **1969**, *18*, 67.
[28] J.-H. So, M. D. Dickey, *Lab Chip* **2011**, *11*, 905.
[29] M. R. Khan, G. J. Hayes, J.-H. So, G. Lazzi, M. D. Dickey, *Appl. Phys. Lett.* **2011**, *99*, 013501.
[30] M. Kubo, X. Li, C. Kim, M. Hashimoto, B. J. Wiley, D. Ham, G. M. Whitesides, *Adv. Mater.* **2010**, *22*, 2749.
[31] J. Park, S. Wang, M. Li, C. Ahn, J. K. Hyun, D. S. Kim, D. K. Kim, J. A. Rogers, Y. Huang, S. Jeon, *Nat. Commun.* **2012**, *3*, 916.
[32] H.-J. Kim, C. Son, B. Ziaie, *Appl. Phys. Lett.* **2008**, *92*, 011904/1.
[33] J.-H. So, H.-J. Koo, M. D. Dickey, O. D. Velev, *Adv. Funct. Mater.* **2011**, *22*, 625.
[34] D. J. Lipomi, B. C. K. Tee, M. Vosgueritchian, Z. Bao, *Adv. Mater.* **2011**, *23*, 1771.
[35] KRATON, G1643 M Polymer, http://docs.kraton.com/tl_warehouse/pdf_data_docs/WG_4140_WG29E4.tmp.pdf (accessed December 2012).
[36] D. Wakuda, K. Suganuma, *Appl. Phys. Lett.* **2011**, *98*, 073304.
[37] J. H. Laurer, R. Bukovnik, R. J. Spontak, *Macromolecules* **1996**, *29*, 5760.